Hiding the which-path information of photons

Jinxian Guo,[1,2,3] Qizhang Yuan,[4,*] Yuan Wu,[5] and Weiping Zhang[1,2,6,3]

[1]*School of Physics and Astronomy, and Tsung-Dao Lee Institute, Shanghai Jiao Tong University, Shanghai 200240, People's Republic of China*

[2]*Shanghai Research Center for Quantum Sciences, Shanghai 201315, People's Republic of China*

[3]*Shanghai Branch, Hefei National Laboratory, Shanghai 201315, People's Republic of China*

[4]*Department of Physics, Mathematics and Science College of Shanghai Normal University, Shanghai 200234, People's Republic of China*

[5]*State Key Laboratory of Precision Spectroscopy, Quantum Institute of Atom and Light, Department of Physics, East China Normal University, Shanghai 200062, People's Republic of China*

[6]*Collaborative Innovation Center of Extreme Optics, Shanxi University, Taiyuan, Shanxi 030006, People's Republic of China*

(Received 15 May 2022; accepted 29 July 2022; published 18 August 2022)

Which-path information of a quantum particle in interferometers is the key to infer the past of the quantum particle. It has led to many extensive discussions, including discussions of quantum complementarity and the path-visibility relation. The basics of these discussions are the description, detection, and control of which-path information. In this paper, we focus on the investigation of multidimensional which-path information in a nested Mach-Zehnder interferometer. A general expression of which-path information is given and can be partially extracted by different detection methods. Further analysis shows that the which-path information can be controlled by the phase differences and beam-splitting ratios between the arms of the nested Mach-Zehnder interferometer. Moreover, an alternative which-path information elimination phenomenon has been predicted and demonstrated experimentally. Our work can help us to understand the physics of quantum particles, with potential applications for quantum information processing and quantum metrology.

DOI: 10.1103/PhysRevA.106.022210

I. INTRODUCTION

Which-path information (WPI) is the information one has about which path a quantum particle took through a device [1,2]. By measuring it in a detector, WPI has been used to infer the past of a quantum particle [3–7]. For example, Wheeler *et al.* [8–10] found a counterfactual result: we cannot infer the past of photons because photons can hide their past. Up to now, WPI is still the key of discussions about basic quantum principles [1,3,4,11–16], including quantum complementarity and the path-visibility relation. These discussions are often accompanied by the elimination of WPI in various interferometers, including double-slit interferometers [3,8,11,12,14] and Mach-Zehnder interferometers (MZIs) [17–27].

Recently, Danan *et al.* found that WPI can be discontinuous [26] in a nested Mach-Zehnder interferometer (NMZI), which has led to extensive discussions [5–7,18–21,24,27–35]. In these discussions, several WPI-elimination phenomena [13,24,27,35] have been pointed out which highly depend on the state of the interferometer, including the stability and relative phases of the interferometer. Are there any other WPI-elimination phenomena? Moreover, the detection method used in NMZIs is a position-sensitive one, which is totally different from Wheeler *et al.*'s case. Is WPI elimination in NMZI related to the detection method? To further understand WPI-elimination phenomena and the underlying physical mechanism, the description, detection, and control of WPI need to be further investigated in NMZI.

In this paper, we use a three-path interference model and focus on the WPI in NMZIs. With the vibrations of mirrors in our interferometer, the position and phase information of photons are changed simultaneously. A general expression for WPI can be obtained which shows multidimensional information. Surprisingly, such multidimensional WPI can be partially extracted by different detection methods. As examples, we use position-sensitive detection and phase-sensitive detection to extract the position- and phase-induced WPI, respectively. Correspondingly, the elimination condition of WPI is reconsidered under a certain detection method. A detailed discussion shows that the WPI can be controlled by the phase differences between the interference arms and the splitting ratios of the beam splitters (BSs) in a NMZI. These results not only explain the experimental results in Ref. [26] but also predict an alternative WPI-elimination phenomenon which is demonstrated experimentally in this paper.

This paper is organized as follows. In Sec. II, a three-path interferometer model is presented with adjustable splitting ratios for the beam splitters, phase differences between the arms, and multiple detection methods. A detailed analysis and discussion of WPI are given in Sec. III. Then we establish an experiment setup and verify the theoretical prediction of the WPI-elimination condition in Sec. IV. The conclusion is given in Sec. V.

II. THEORETICAL MODEL

Our model is shown in Fig. 1; photons are emitted from the laser source and enter the interferometer.

*lphysics@shnu.edu.cn

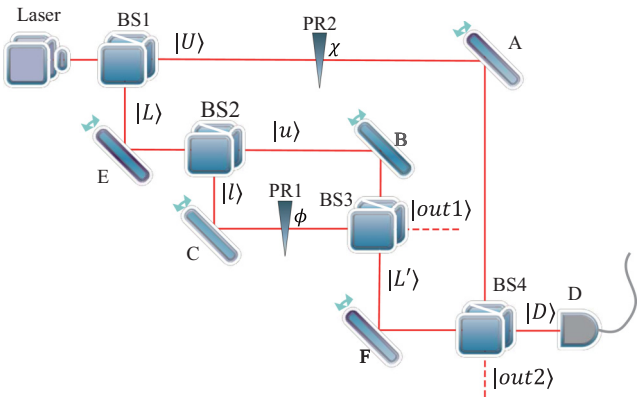

FIG. 1. Scheme of NMZI. All the splitting ratios of the beam splitters (BSs) used in this NMZI are adjustable. Mirrors A, B, C, E, and F vibrate with different frequencies $f_k, k = a, b, c, e, f$. PR1 and PR2 represent the phase retarders, and D is the photon detector.

Different from previous work, the interferometer is built by BSs with adjustable beam-splitting ratios. The mirrors in the interferometer [5–7,21,24,27,32–35] oscillate slightly with distinguishable frequencies f_k which introduce additional complex phase shifts φ_k, where $k = a, b, c, e, f$. The real part and imaginary part of φ_k represent the change in the optical phase and position of the light beam caused by the vibration [27,35], respectively. The WPI of photons is indicated by φ_k, which can be extracted in the detector. For example, if we recognize φ_a in the detector, we know that the photons have been reflected by mirror A. To control the WPI, we introduce two phase shifts, ϕ and χ, using the tunable phase retarders (PR1 and PR2, as shown in Fig. 1; no intensity attenuation is introduced) when photons pass through the interferometer on three different paths.

In detail, when photons are emitted from the light source, the photon state passing through BS1 is

$$|\psi_1\rangle = t_1|U\rangle + ir_1|L\rangle, \tag{1}$$

where t_1 is the amplitude transmissivity of BS1 and $r_1 = \sqrt{1-t_1^2}$ is the corresponding amplitude reflectivity. Here $|L\rangle$ is the photon state reflected by BS1 going through the lower arm of the outer MZI, while $|U\rangle$ is the photon state propagating along the upper arm of MZI through BS1.

Similarly, after photons pass through mirror E and BS2 of the inner MZI, the state changes to

$$\begin{aligned}|\psi_2\rangle = {} & t_1 e^{i\varphi_a} e^{i\chi}|U\rangle + ir_1 t_2 e^{i(\varphi_b+\varphi_e)}|u\rangle \\ & -r_1 r_2 e^{i(\varphi_c+\varphi_e)} e^{i\phi}|l\rangle,\end{aligned} \tag{2}$$

where $\varphi_k, k = a, b, c, e$, are the tiny complex phases caused by the vibration of mirrors A, B, C, and E. The mirrors we use here are highly reflective and have no loss. State $|l\rangle$ is the photon state reflected by BS2 with amplitude reflectivity r_2 propagating along the lower arm of the internal MZI. State $|u\rangle$ is transmitted by BS2 with amplitude transmissivity $t_2 = \sqrt{1-r_2^2}$ and propagates along the upper arm of the inner MZI. Due to PR1 and PR2, we introduce two phase shifts, ϕ and χ, into the state. Here ϕ is the real phase difference between the two arms of the internal interferometer, while χ is the real phase difference between the two arms of the outer interferometer.

When photons pass through the beam combiner (BS3) in the internal MZI, the state of the photons becomes

$$\begin{aligned}|\psi_3\rangle = {} & -(r_1 t_2 r_3 e^{i(\varphi_e+\varphi_b)} + r_1 r_2 t_3 e^{i(\varphi_e+\varphi_c)} e^{i\phi})|\text{out1}\rangle \\ & -i(r_1 r_2 r_3 e^{i(\varphi_e+\varphi_c)} e^{i\phi} - r_1 t_2 t_3 e^{i(\varphi_e+\varphi_b)})|L'\rangle \\ & +t_1 e^{i\varphi_a} e^{i\chi}|U\rangle,\end{aligned} \tag{3}$$

where t_3 and $r_3 = \sqrt{1-t_3^2}$ are the amplitude transmissivity and reflectivity of BS3, respectively. State $|L'\rangle$ refers to the state in which photons propagate along the lower arm of the external MZI and reach mirror F after beam combination. State |out1⟩ denotes that photons leave NMZI without being detected.

After BS4, the final photon state from the interferometer is

$$|\psi_4\rangle = p_d|D\rangle + p_{o1}|\text{out1}\rangle + p_{o2}|\text{out2}\rangle, \tag{4}$$

where p_d, p_{o1}, and p_{o2} are the probability amplitudes,

$$p_d = it_1 r_4 e^{i\chi} e^{i\varphi_a} - ir_1 t_4 [r_2 r_3 e^{i(\varphi_e+\varphi_c)} e^{i\phi} - t_2 t_3 e^{i(\varphi_e+\varphi_b)}] e^{i\varphi_f} \tag{5}$$

$$p_{o1} = -[r_1 t_2 r_3 e^{i(\varphi_e+\varphi_b)} + r_1 r_2 t_3 e^{i(\varphi_e+\varphi_c)} e^{i\phi}] \tag{6}$$

$$p_{o2} = t_1 t_4 e^{i\varphi_a} e^{i\chi} + r_1 r_4 [r_2 r_3 e^{i(\varphi_e+\varphi_c)} e^{i\phi} - t_2 t_3 e^{i(\varphi_e+\varphi_b)}] e^{i\varphi_f}. \tag{7}$$

Here t_4 and $r_4 = \sqrt{1-t_4^2}$ are the amplitude transmissivity and reflectivity of BS4. State $|D\rangle$ is the photon state finally received by detector D, while state |out2⟩ indicates that photons are not detected after passing through the NMZI. Then we can obtain the probability of the photons reaching the detector as $P_D = |p_d|^2$. Following the three-path interference model [27,35], the complex phases caused by mirror vibrations are usually very small. Under such a condition, we can make the linear approximation $e^{i\varphi_k} \approx 1 + i\varphi_k$, where $k = a, b, c, e, f$. Then the probability can be simplified to

$$\begin{aligned}P_D \approx {} & -2\text{Im}[(\alpha e^{-i\chi} + \beta - \gamma e^{-i\phi})(\alpha\varphi_a e^{i\chi} + \beta\varphi_b - \gamma\varphi_c e^{i\phi})] \\ & -2\text{Im}[(\alpha e^{-i\chi} + \beta - \gamma e^{-i\phi})(\beta - \gamma e^{i\phi})(\varphi_e + \varphi_f)] \\ & +|\alpha e^{i\chi} + \beta - \gamma e^{i\phi}|^2,\end{aligned} \tag{8}$$

where $\alpha = t_1 r_4$, $\beta = r_1 t_2 t_3 t_4$, and $\gamma = r_1 r_2 r_3 t_4$ are the amplitudes of the three paths through the interferometer to output $|D\rangle$. Here we keep only the linear terms of the complex phase and neglect the high-order terms. This is the general output of the NMZI, which is highly related to the splitting ratios and relative phases ϕ and χ.

The general probability shows that all the WPI caused by vibrating mirrors has reached the detector. And the probability consists of complex phases which have two dimensions of information, phase-sensitive $\text{Re}(\varphi_k)$ and position-sensitive $\text{Im}(\varphi_k)$. Such multiple-dimensional information can be extracted by detection. Proper detection, such as a quad-cell detector with both the difference and sum computation of the signals from each cell, can extract the full information, including both parts $\text{Re}(\varphi_k)$ and $\text{Im}(\varphi_k)$. The interesting thing is that the WPI can also be partially extracted, which is not simply

proportional to the probability P_D. For example, Ref. [26] used a position-sensitive quad-cell photodetector to receive the signal. The photons enter the four cells and generate four currents (i_j, $j = 1, 2, 3, 4$) containing the same interference fringes with different intensities which depend on the photon positions (see Appendix A for details). Then we can obtain the position-sensitive signal $i_{\rm pos} = i_1 + i_2 - i_3 - i_4$, which contains no interference fringes caused by the optical phase [the real part of complex phases $\mathrm{Re}(\varphi_k)$, $k = a, b, c, e, f$] and is sensitive to only the signal caused by the position, i.e., the imaginary part $\mathrm{Im}(\varphi_k)$. That is to say, the position-sensitive signal $i_{\rm pos}$ is proportional to the $\mathrm{Im}(\varphi_k)$ parts in Eq. (8) as

$$\begin{aligned} i_{\rm pos} \approx & -2[\beta^2 + \gamma^2 - 2\beta\gamma\cos\phi + \alpha\beta\cos\chi - \alpha\gamma\cos(\phi - \chi)] \\ & \times[\mathrm{Im}(\varphi_e) + \mathrm{Im}(\varphi_f)] \\ & -2\alpha[\alpha + \beta\cos\chi - \gamma\cos(\phi - \chi)]\mathrm{Im}(\varphi_a) \\ & -2\beta[\alpha\cos\chi + \beta - \gamma\cos(\phi)]\mathrm{Im}(\varphi_b) \\ & +2\gamma[\alpha\cos(\phi - \chi) + \beta\cos\phi - \gamma]\mathrm{Im}(\varphi_c). \end{aligned} \tag{9}$$

Noticeably, both parts of the complex phases can tell us the WPI. Assuming that the laser beam's waist is large enough, the term with $\mathrm{Im}(\varphi_k)$ can be considered to be much smaller than the terms with $\mathrm{Re}(\varphi_k)$ (see Appendix A for details). Then with a single-pixel detector, we can obtain interference fringes caused by only phase terms $\mathrm{Re}(\varphi_k)$. The corresponding phase-sensitive signal $i_{\rm pha}$ is proportional to the real part $\mathrm{Re}(\varphi_k)$ in Eq. (8) as

$$\begin{aligned} i_{\rm pha} \approx & \, 2\alpha[\beta\sin\chi + \gamma\sin(\phi - \chi)][\mathrm{Re}(\varphi_e) + \mathrm{Re}(\varphi_f)] \\ & -2\alpha[\beta\sin\chi + \gamma\sin(\phi - \chi)]\mathrm{Re}(\varphi_a) \\ & +2\beta[\alpha\sin\chi - \gamma\sin(\phi)]\mathrm{Re}(\varphi_b) \\ & +2\gamma[\alpha\sin(\phi - \chi) + \beta\sin\phi]\mathrm{Re}(\varphi_c), \end{aligned} \tag{10}$$

where we neglect the terms without complex phases. Obviously, the WPI extracted by phase-sensitive detection is totally different from the position-sensitive WPI. In the following section, we reconsider the elimination conditions of WPI according to the detection-dependent WPI, i.e., the absence of phases related to the vibrating mirrors in detector D.

III. ANALYSIS AND DISCUSSION

For simplicity, we start the analysis with the elimination of WPI caused by only mirror A. When using position-sensitive detection, the terms with $\mathrm{Im}(\varphi_a)$ in Eq. (9) are $-2\alpha[\alpha + \beta\cos\chi - \gamma\cos(\phi - \chi)]\mathrm{Im}(\varphi_a)$. Since the vibration of mirror A always causes a position change and the light reflected by mirror A is not zero, we set $\mathrm{Im}(\varphi_a) \neq 0$ and $\alpha \neq 0$. Then to eliminate WPI of mirror A by position-sensitive detection, the beam-splitting ratios of the BSs and phase shifts of the NMZI should satisfy

$$\alpha + \beta\cos\chi - \gamma\cos(\phi - \chi) = 0. \tag{11}$$

As we can see, the elimination condition of mirror A contains α, β, and γ, which means that the three paths are interfering simultaneously when using position-sensitive detection. To eliminate the position-induced WPI of mirror A, the photons coming from path $|U\rangle$ should be totally eliminated by the interference, while the photons from the other two paths can still exist, making the output power at the detector proportional to $\beta\sin\chi + \gamma\sin(\phi - \chi)$. At this time, if we use another position-sensitive detection at the output $|\mathrm{out2}\rangle$, we can obtain the condition to eliminate the position-sensitive WPI of mirror A as $t_1t_4 - r_1r_4[t_2t_3\cos\chi - r_2r_3\cos(\chi - \phi)] = 0$ (see Appendix B for details). The interesting thing is that this condition can be achieved even when $\alpha + \beta\cos\chi - \gamma\cos(\chi - \phi) = 0$, for example, when $t_1 = \sqrt{1/3}$, $t_2 = t_3 = t_4 = \sqrt{1/2}$. That is to say, the position-sensitive WPI of mirror A can be eliminated at both outputs $|\mathrm{out2}\rangle$ and $|D\rangle$, while the phase-sensitive WPI is hidden by the detectors.

But if we use phase-sensitive detection, the elimination condition of WPI is different. With phase-sensitive detection, we can get only the real part of the complex phase. Then the WPI caused by mirror A can also be eliminated at output $|D\rangle$ when

$$\beta\sin\chi + \gamma\sin(\phi - \chi) = 0. \tag{12}$$

As we can see, there is no α in this condition, which is quite different from the position-detection case. This is because of the different detection methods. Actually, the phase information $\mathrm{Re}(\varphi_a)$ can be extracted only from interference fringes. The absence of α in Eq. (12) is induced by a destructive interference of the inner MZI at path $|L'\rangle$ which erases the WPI from path $|U\rangle$. Then no interference fringes can be detected at detector D, which erases the WPI of mirror A when using phase-sensitive detection. This can never happen when using the position-sensitive method since position-induced WPI can be detected even with only one path of light reaching the detector. In this case, there are also no interference fringes at output $|\mathrm{out2}\rangle$, which means that the WPI of mirror A is detected at all the outputs using phase-sensitive detection. Therefore, the elimination condition of WPI completely depends on the method of detection. In other words, mirror vibration has multidimensional information, which causes the WPI to have a variety of presentations according to different detection methods.

On the other hand, elimination of the WPI of mirror A is due to the interference of multiple paths. In NMZIs, interference may occur between any two of the three paths or simultaneously between the three paths. So many kinds of interference happening in NMZIs result in multiple WPI-elimination phenomena. Along these lines, we can further obtain the conditions for eliminating WPI caused by mirrors B, C, E, and F from Eq. (9), as shown in Table I. As we can see, the conditions using position-sensitive detection can explain the experimental result of Ref. [26]. Moreover, Table I shows that WPI resulting from any mirrors can be eliminated under certain conditions, except for erasing all the WPI simultaneously since erasing all the WPI simultaneously means that no photon can reach the detector, which is a meaningless result.

Combining the multipath interference and the detection-dependent WPI, the WPI-elimination effect becomes richer and more controllable than in previous studies [18,26,35]. In previous work [18,19,35], the WPI caused by mirrors E and F was eliminated simultaneously, while the WPI of mirrors A, B, and C remained. In our case, Table I shows that WPI caused by any two mirrors can be eliminated at the same time, not only that caused by mirrors E and F. What we need to do is to

TABLE I. The conditions for eliminating WPI of photons caused by vibrating mirrors.

WPI to be eliminated	Condition	Detection method
$\mathrm{Im}(\varphi_a)$	$\alpha+\beta\cos\chi-\gamma\cos(\phi-\chi)=0$	position sensitive
$\mathrm{Re}(\varphi_a)$	$\beta\sin\chi+\gamma\sin(\phi-\chi)=0$	phase sensitive
$\mathrm{Im}(\varphi_b)$	$\alpha\cos\chi+\beta-\gamma\cos\phi=0$	position sensitive
$\mathrm{Re}(\varphi_b)$	$\alpha\sin\chi-\gamma\sin\phi=0$	phase sensitive
$\mathrm{Im}(\varphi_c)$	$\alpha\cos(\phi-\chi)+\beta\cos\phi-\gamma=0$	position sensitive
$\mathrm{Re}(\varphi_c)$	$\alpha\sin(\phi-\chi)+\beta\sin\phi=0$	phase sensitive
$\mathrm{Im}(\varphi_e)$ and $\mathrm{Im}(\varphi_f)$	$\beta^2+\gamma^2-2\beta\gamma\cos\phi+\alpha\beta\cos\chi-\alpha\gamma\cos(\phi-\chi)=0$	position sensitive
$\mathrm{Re}(\varphi_e)$ and $\mathrm{Re}(\varphi_f)$	$\beta\sin\chi+\gamma\sin(\phi-\chi)=0$	phase sensitive

carefully adjust the phase differences and the beam-splitting ratios of the BSs which satisfy multiple equations in Table I at the same time. Thus, we can simultaneously eliminate the WPI caused by three mirrors, A, E, and F, according to Table I. As we can see in Table I, the elimination conditions of $\mathrm{Re}(\varphi_a)$, $\mathrm{Re}(\varphi_e)$, and $\mathrm{Re}(\varphi_f)$ are the same, which means that they can be eliminated together. In this case, the light coming from the laser source can still reach the detector but contains WPI of only mirrors B and C. Such a phenomenon is due to not only the three-path interference but also the usage of the phase-sensitive detection method, which is hardly seen in previous work [18,24,26,27,35].

IV. EXPERIMENTAL RESULTS

To verify the above results, we set up an experiment with phase-sensitive detection as shown in Fig. 2. A 1-mW, 795-nm monocolor continuous laser from a distributed feedback laser diode is injected into an interferometer. To avoid detecting the signal caused by imaginary parts of complex phases, we use a Gaussian beam with a beam waist of 2 mm. Such a large beam waist ensures that the interference fringes we detected are caused by only $\mathrm{Re}(\varphi_k), k=a,b,c,e,f$, as stated in the Appendix A. The light is first separated into the two arms of the interferometer with different polarizations by a half-wave plate (HWP1) and a polarization beam splitter (PBS1), as shown in Fig. 2. The combination of the half-wave plate and PBS acts as an adjustable beam splitter. By changing the angle of HWP1, the laser power in the two arms varies. Then the light is reflected by the mirrors driven by piezoelectric transducers (PZTs) [26]. As shown in Fig. 2, each $\mathrm{PZT}_k, k=a,b,c,e,f$, is driven by a wave-form generator which makes each mirror vibrates at different frequencies $f_k, k=a,b,c,e,f$.

After passing through the inner interferometer, the laser beams are combined by PBS3 with two orthogonal polarizations, as shown in Fig. 2. To make two such orthogonal polarized lights interfere, we use HWP3 to rotate the two lights' polarizations and then use PBS4 to divide them into horizontal and vertical polarization components. As a result, two beams are mixed in both vertical polarization and horizontal polarizations after PBS4. Such PBSs with a HWP act as an adjustable beam combiner. The same combination is used in the outer interferometer to get the final output. A single-pixel detector, D1, is used to detect the output of interferometer. The final output signal of D1 is analyzed by a power spectrum analyzer to obtain the WPI of photons.

According to Table I, the two relative phases, ϕ and χ, play central roles in eliminating the WPI. So the two phases of the NMZI should be accurately controlled and simultaneously detected without affecting WPI. To control phases ϕ and χ, we use corner prisms with PZT6 and PZT7 (as shown in the dashed boxes in Fig. 2) as phase retarders which can adjust the relative optical lengths without changing the visibility of the interference fringes. Then we use another two detectors, D2 and D3, to measure the two phases by acquiring the

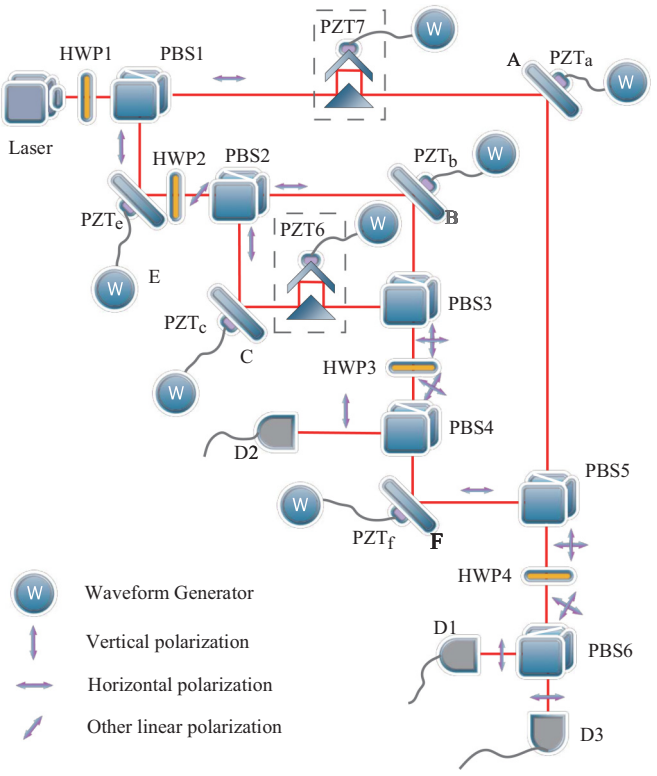

FIG. 2. Experimental setup of NMZI. HWP: half-wave plate; PBS: polarization beam splitter; D: detectors; PZT: piezoelectric transducer. The light coming from the laser source passes through the NMZI with different polarizations. Each mirror in the NMZI can vibrate with a PZT that is controlled by a wave-form generator. Mirrors A, B, C, E, and F vibrate with $\mathrm{PZT}_k, k=a,b,c,e,f$, whose frequencies are $f_a=1.1$ kHz, $f_b=1.2$ kHz, $f_c=1.3$ kHz, $f_e=1.4$ kHz, and $f_f=1.5$ kHz, respectively. The arrows represent the polarization directions of the light. Inside the two dashed boxes are the phase retarders built by the corner prisms.

interference signals of photon states $|\text{out1}\rangle$ and $|\text{out2}\rangle$. As shown in Fig. 2, D2 is used to measure photon state $|\text{out1}\rangle$, the interference signal of the inner interferometer. And D3 is used to measure photon state $|\text{out2}\rangle$, an output of the outer interferometer. Such interference signals contain the phase information of the NMZI when the vibrations of the mirror are small enough. According to Eqs. (6) and (7), we can obtain the relation between phases ϕ and χ and the beam-splitting ratios r_n, $n = 1, 2, 3, 4$, through the possibilities of $P_{D2} = |p_{o1}|^2$ and $P_{D3} = |p_{o2}|^2$. Then by neglecting the small vibrations of the interference fringes caused by the mirrors, we can derive the two phases as

$$\phi = \cos^{-1}\left[\frac{P_{D2} - r_1^2\left(t_2^2 r_3^2 + r_2^2 t_3^2\right)}{2r_1^2 t_2 r_2 t_3 r_3}\right], \tag{13}$$

$$\chi = \cos^{-1}\frac{P_{D3} - \left(t_1^2 t_4^2 + r_1^2 r_2^2 r_3^2 r_4^2 + r_1^2 t_2^2 t_3^2 r_4^2 - 2r_1^2 r_2 t_2 r_3 t_3 r_4^2 \cos\phi\right)}{2r_1 t_1 r_4 t_4 \sqrt{r_2^2 r_3^2 + t_2^2 t_3^2 - 2r_2 r_3 t_2 t_3 \cos\phi}} - \theta, \tag{14}$$

where P_{D2} and P_{D3} can be obtained with optical powers detected by D2 and D3 which are normalized to the input power and

$$\theta = \cos^{-1}\frac{(r_2 r_3 \cos\phi - t_2 t_3)}{\sqrt{r_2^2 r_3^2 + t_2^2 t_3^2 - 2r_2 r_3 t_2 t_3 \cos\phi}}. \tag{15}$$

In our experiment, by tuning the angle of HWPs before each PBS, we can easily achieve the adjustment of beam-splitting ratios. Then we can adjust the control voltages of PZT6 and PZT7 to change phases ϕ and χ. When we adjust the HWPs to set $r_1 = t_4 = \sqrt{2/3}$, $r_2 = r_3 = \sqrt{1/2}$, the intensities of the light fields in the three paths of the NMZI are the same. By varying phases ϕ and χ, we can observe the elimination of WPI caused by mirrors A, B, and C and E and F in experiment (as shown in Fig. 3). By using Eqs. (13)–(15), the elimination conditions of WPI caused by mirrors A, E, and F [as shown in Fig. 3(a)] in experiment are $\phi = 0.15$ rad and $\chi = 1.67$ rad, consistent with Eq. (12). When the phases of the inner and outer interferometers become $\phi = 1.31$ rad and $\chi = 0.48$ rad in experiment, the WPI caused by mirror B is eliminated, as shown in Fig. 3(b). Moreover, the WPI of mirror C is eliminated, as shown in Fig. 3(c), if the two phases are $\phi = 0.74$ rad and $\chi = 1.11$ rad. Such experimental results are all consist with the predictions in Table I.

Furthermore, we experimentally demonstrate the elimination of WPI with different beam-splitting ratios in the NMZI. Changing the angle of HWP2, the splitting ratio of PBS2 varies. Then to eliminate the WPI of mirror A, we should vary the voltage of PZT6 and PZT7 to change phases ϕ and χ. As shown in Fig. 4, the red circles are experimentally recorded phases ϕ and χ when eliminating WPI of mirrors A, E, and F at $r_2 = 0.447$. As we can see, phases ϕ and χ vary together and fit well with the theoretical simulation (the solid blue line). When the splitting ratio $r_2 = 0.836$, the relation between the two phases changes, as shown by the yellow stars in Fig. 4. Also, the relation is consistent with the corresponding theoretical simulation (dashed black line in Fig. 4). These results prove that our theoretical analysis is in good agreement with the experimental facts.

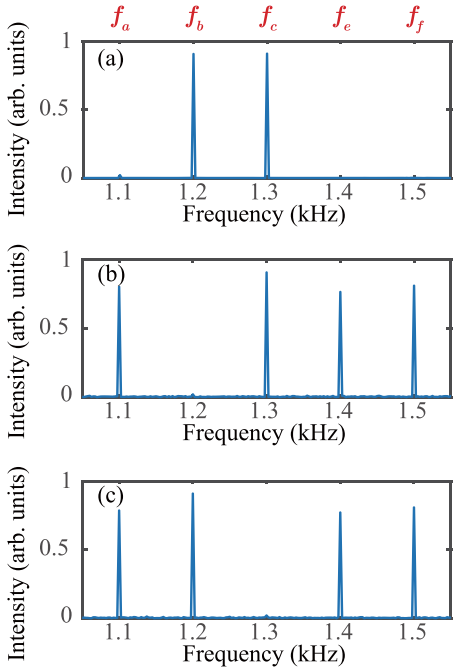

FIG. 3. The experimental power spectrum of the photon current from D1 shows the elimination of WPI from (a) mirrors A, E, and F, (b) mirror B, and (c) mirror C with phase-sensitive detection.

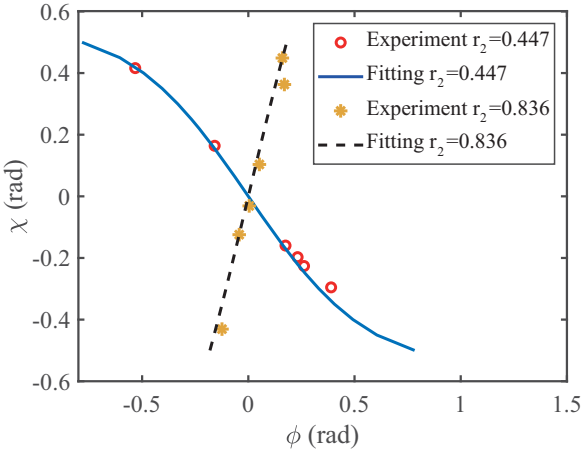

FIG. 4. The experimental phase conditions to eliminate WPI of mirrors A, E, and F by phase-sensitive detection. The symbols are the experimental data, and the lines are the corresponding fittings. As we can see, the relation between the two phases ϕ and χ varies with the splitting ratio r_2 of PBS2 and fits the theoretical predictions.

V. CONCLUSION

In summary, we revisited the three-path interference problem which gives the general expression of photons' WPI in NMZIs. This general result not only can explain the previous experimental results but also predicted an alternative WPI-elimination phenomenon. More importantly, we proposed that there are two kinds of WPI, which relate to the real and imaginary parts of the complex phase and can be detected by different detection methods. One uses phase-sensitive detection, which receives only the real-part-related WPI. The other one uses position-sensitive detection to measure the imaginary-part-related WPI without receiving the real-part-related WPI. Due to the different presences of WPI, we discovered a different method to eliminate WPI by controlling the beam-splitting ratio and phases of the interferometer.

Our results can help us to understand the physics of quantum particles. Moreover, such a detection-dependent WPI-elimination phenomenon may potentially be used in quantum information process, such as multichannel quantum communication. The phase-sensitive part and the position-sensitive part of the WPI can potentially be used as two individual channels for the quantum information, causing the photons to contain multidimensional information. Thanks to the wide application of NMZIs [36,37], some results in this paper may also be applied to quantum metrology. For example, the WPI-elimination method is helpful to develop an anti-interference interferometer which can realize the sensing of specific phase information and avoid the disturbance of other stray signals. Moreover, using position-sensitive detection to lock the NMZI while using phase-sensitive detection for the metrology may be a quite useful technical application.

ACKNOWLEDGMENTS

We acknowledge financial support from the Innovation Program for Quantum Science and Technology (Grant No. 2021ZD0303200), the National Key Research and Development Program of China (Grant No. 2016YFA0302001), the National Science Foundation of China (Grants No. 11904227, No. 12104161, No. 11804225, and No. 11654005), the Sailing Program of Shanghai Science and Technology Committee under Grants No. 19YF1421800 and No. 19YF1414300, and the Shanghai Municipal Science and Technology Major Project (Grant No. 2019SHZDZX01). W.Z. also acknowledges additional support from the Shanghai talent program.

APPENDIX A: POSITION-SENSITIVE DETECTION AND PHASE-SENSITIVE DETECTION

To simply demonstrate the position-sensitive-detection and phase-sensitive-detection methods, we set the problem in a normal MZI. Considering a Gaussian light with $\Psi(x,y) = A_0\exp[-(x^2+y^2)/2\Delta^2]$ reflected by a vibrating mirror, where A_0 is the amplitude of light and Δ is the beam waist, the complex phase makes the field become $\Psi(x,y) = A_0\exp\{-[x^2+(y+\delta))]^2\}/2\Delta^2]\exp(i\phi)$, where δ and ϕ are the position shift and phase shift caused by mirror vibration. With the tiny-vibration assumption, we can keep only the first-order term [26], which gives light $\Psi(x,y) = A_0\exp[-(x^2+y^2)/2\Delta^2]\exp(-y\delta/2\Delta^2)\exp(i\phi)$. Obviously, the complex phase shift is $\varphi = \phi + iy\delta/2\Delta^2$. Then the interference term is

$$2A_0^2 e^{-\frac{x^2+y^2}{\Delta^2}} e^{-\frac{y\delta}{2\Delta^2}}\cos\phi \approx 2A_0^2 e^{-\frac{x^2+y^2}{\Delta^2}}\left(1-\frac{y\delta}{2\Delta^2}\right)\cos\phi. \quad \text{(A1)}$$

For the position-sensitive detection, a quad-cell detector was used which can obtain four currents i_j as

$$i_1 = i_2 = \frac{1}{2}A_0^2 e^{-\frac{x^2+y^2}{\Delta^2}}\left(1+\frac{y\delta}{2\Delta^2}\right)\cos\phi, \quad \text{(A2)}$$

$$i_3 = i_4 = \frac{1}{2}A_0^2 e^{-\frac{x^2+y^2}{\Delta^2}}\left(1-\frac{y\delta}{2\Delta^2}\right)coas\phi. \quad \text{(A3)}$$

Then the position-sensitive current $i_{\rm pos}$ is

$$i_{\rm pos} = A_0^2 e^{-\frac{x^2+y^2}{\Delta^2}}\frac{y\delta}{\Delta^2}\cos\phi, \quad \text{(A4)}$$

which is proportional to the position-sensitive term $\mathrm{Im}(\varphi)$.

For phase-sensitive detection, a large beam waist $\Delta \gg \delta_a$ is used. We can neglect the term $y\delta/2\Delta^2$, which means the detector can see only the phase-sensitive interference fringes and gives the phase sensitive signal

$$i_{\rm pha} \approx 2A_0^2\exp[-(x^2+y^2)/\Delta^2]\cos\phi. \quad \text{(A5)}$$

That is why a single-pixel detector and a large beam waist can achieve phase-sensitive detection. Although we are discussing only a very simple case, the relevant assumptions and conclusions are not difficult to extend to complex cases, such as in NMZI.

APPENDIX B: WPI IN OUTPUT 2

According to the output equation (7), we can obtain the probability of photons reaching output 2 as $P_{\rm out2} = |p_{o2}|^2$. Similar to output $|D\rangle$, we can also apply position-sensitive detection and phase-sensitive detection at output $|\mathrm{out2}\rangle$, which gives the position-sensitive signal and phase-sensitive signal of mirror A as

$$i_{o2,\mathrm{pos},A} \propto \{t_1t_4 - r_1r[t_2t_3\cos\chi - r_2r_3\cos(\phi-\chi)]\}\mathrm{Im}(\varphi_a), \quad \text{(B1)}$$

$$i_{o2,\mathrm{pha},A} \propto [r_2r_3\sin(\phi-\chi) + t_2t_3\sin\chi]\mathrm{Re}(\varphi_a), \quad \text{(B2)}$$

where we also neglect the terms without complex phases. As we can see, to eliminate the WPI of mirror A by position-sensitive detection we should keep

$$t_1t_4 - r_1r_4[t_2t_3\cos\chi - r_2r_3\cos(\chi-\phi)] = 0. \quad \text{(B3)}$$

When using phase-sensitive detection at output $|\mathrm{out2}\rangle$, the condition to eliminate the phase-sensitive WPI of mirror A becomes

$$r_2r_3\sin(\phi-\chi) + t_2t_3\sin\chi = 0, \quad \text{(B4)}$$

which is the same as the condition at output $|D\rangle$. The other conditions can also be derived with the same method, which shows many detection-dependent WPI-elimination phenomena.

[1] E. Bagan, J. A. Bergou, S. S. Cottrell, and M. Hillery, Phys. Rev. Lett. **116**, 160406 (2016).
[2] J. S. Lundeen, Physics **6**, 133 (2013).
[3] P. Storey, S. Tan, M. Collett, and D. Walls, Nature (London) **367**, 626 (1994).
[4] S. Dürr, T. Nonn, and G. Rempe, Nature (London) **395**, 33 (1998).
[5] V. Potoček and G. Ferenczi, Phys. Rev. A **92**, 023829 (2015).
[6] R. B. Griffiths, Phys. Rev. A **94**, 032115 (2016).
[7] H. Geppert-Kleinrath, T. Denkmayr, S. Sponar, H. Lemmel, T. Jenke, and Y. Hasegawa, Phys. Rev. A **97**, 052111 (2018).
[8] J. A. Wheeler, in *Mathematical Foundations of Quantum Theory*, edited by A. Marlow (Academic, Oxford, 1978), pp. 9–48.
[9] J. A. Wheeler, *Quantum theory and measurement* (Princeton University Press, Princeton, NJ, 1984), pp. 182–213.
[10] V. Jacques, E. Wu, F. Grosshans, F. Treussart, P. Grangier, A. Aspect, and J.-F. Roch, Science **315**, 966 (2007).
[11] M. Scully, B. Englert, and H. Walter, Nature (London) **351**, 111 (1991).
[12] A. J. Leggett, *Compendium of Quantum Physics* (Springer, Berlin, 2009), pp. 161–166.
[13] T. J. Herzog, P. G. Kwiat, H. Weinfurter, and A. Zeilinger, Phys. Rev. Lett. **75**, 3034 (1995).
[14] Z.-Y. Zhou, Z.-H. Zhu, S.-L. Liu, Y.-H. Li, S. Shi, D.-S. Ding, L.-X. Chen, W. Gao, G.-C. Guo, and B.-S. Shi, Sci. Bull. **62**, 1185 (2017).
[15] J. Gao, Z.-Q. Jiao, C.-Q. Hu, L.-F. Qiao, R.-J. Ren, H. Tang, Z.-H. Ma, S.-M. Fei, V. Vedral, and X.-M. Jin, Commun. Phys. **1**, 89 (2018).
[16] M. Lahiri, Phys. Rev. A **83**, 045803 (2011).
[17] A. Peruzzo, P. Shadbolt, N. Brunner, S. Popescu, and J. L. O'Brien, Science **338**, 634 (2012).
[18] L. Vaidman, Phys. Rev. A **87**, 052104 (2013).
[19] L. Vaidman, Phys. Rev. A **89**, 024102 (2014).
[20] L. Vaidman and I. Tsutsui, Entropy **20**, 538 (2018).
[21] G. N. Nikolaev, JETP Lett. **105**, 152 (2017).
[22] T. Hellmuth, H. Walther, A. Zajonc, and W. Schleich, Phys. Rev. A **35**, 2532 (1987).
[23] B.-G. Englert, K. Horia, J. Dai, Y. L. Len, and H. K. Ng, Phys. Rev. A **96**, 022126 (2017).
[24] M. A. Alonso and A. N. Jordan, Quantum Stud.: Math. Found. **2**, 255 (2015).
[25] D. Sokolovski, Phys. Lett. A **381**, 227 (2017).
[26] A. Danan, D. Farfurnik, S. Bar-Ad, and L. Vaidman, Phys. Rev. Lett. **111**, 240402 (2013).
[27] Q. Yuan and X. Feng, Chin. Opt. Lett. **19**, 012701 (2021).
[28] L. Vaidman, Phys. Rev. A **93**, 017801 (2016).
[29] L. Vaidman, Phys. Rev. A **95**, 066101 (2017).
[30] L. Vaidman, arXiv:1806.01774.
[31] L. Vaidman, JETP Lett. **105**, 473 (2017).
[32] Z.-H. Li, M. Al-Amri, and M. S. Zubairy, Phys. Rev. A **88**, 046102 (2013).
[33] F. A. Hashmi, F. Li, S.-Y. Zhu, and M. S. Zubairy, J. Phys. A **49**, 345302 (2016).
[34] F. A. Hashmi, F. Li, S.-Y. Zhu, and M. S. Zubairy, J. Phys. A **51**, 068001 (2018).
[35] Q. Z. Yuan and X. Feng, Phys. Rev. A **99**, 053805 (2019).
[36] W. Du, J. Kong, G. Bao, P. Yang, J. Jia, S. Ming, C.-H. Yuan, J. F. Chen, Z. Y. Ou, M. W. Mitchell, and W. Zhang, Phys. Rev. Lett. **128**, 033601 (2022).
[37] W. Du, J. F. Chen, Z. Y. Ou, and W. Zhang, Appl. Phys. Lett. **117**, 024003 (2020).